www.rericjournal.ait.ac.th

A Novel Optimal Control Strategy for Energy Management in a Hybrid Microgrid System

Saritha K.S.*, [1], Sasidharan Sreedharan[#], and Usha Nair*

ARTICLE INFO

Article history:
Received 27 July 2022
Received in revised form
16 January 2023 (1st revision)
26 January 2023 (2nd revision)
Accepted 28 March 2023

Keywords:
Control strategy
Energy management
Hybrid microgrid
Optimization
Stability

ABSTRACT

This paper presents an optimal control technique for cost-effective microgrid operation that guarantees system stability in both off-grid and on-grid modes. This work proposes an evolutionary algorithmic approach to increasing power generation from renewable energy sources while minimizing losses. The system's loadability is enhanced, and general system limits and stability requirements such as the line stability index, voltage stability index, and small-signal stability are taken into account to achieve the best possible penetration of renewable energy. The proposed control method is employed in a campus microgrid and a microgrid integrated with the Indian (Kerala) power system. In off-grid mode, the renewable energy penetration into the microgrid is boosted to 87.5% more than the base scenario by enhancing system loadability to 94.9%, while in on-grid mode, the renewable power contribution improves by 46% more than the base scenario with an additional 9.4% of loadability. The results demonstrate that by maximizing renewable penetration, reducing power losses, and ensuring system stability in both off-grid and on-grid modes, a cost-effective and stable microgrid operation is achieved. Furthermore, grid integration and optimal loading enhance system performance.

1. INTRODUCTION

Providing consumers with adequate, reliable, and economical electric power is the primary objective of any power system. The power sector is changing dramatically around the world as a result of ever-growing electric power demand, increased deployment of clean renewable energy sources, and the increasing prevalence of grid-connected distributed generation. Many types of research are being conducted in the power system field to modernize the conventional system and also in energy management techniques. Energy management (EM) is an essential strategy in the power sector to provide cost-effective, quality power to consumers. A low-voltage (LV) distribution network's impact on a renewable integrated microgrid (MG) is explored in [1]. The distributed energy management control architecture and multi-objective optimization are described in [2]. An analysis of the economic characteristics of solar PV plants revealed that the PV module cost accounts for a significant portion of the overall investment [3]. Fortunately, the cost of a solar PV system is currently more economically competitive than in the past with conventional power sources.

Microgrids (MGs) are the most cost-effective and efficient way to provide power in isolated or rural locations where grid extension is difficult or impossible. Demand-side management is the most cost-effective strategy to reduce carbon emissions, and it would outperform renewable support instruments [4]. The cost of a microgrid is significantly influenced by conventional sources, particularly combined heat and power [5].

Many multi-objective optimization approaches, such as Multi-Objective Particle Swarm optimization (MOPSO), Non-dominated Sorting Genetic Algorithm (NSGA-II), Genetic Algorithm (GA), Self-adaptive low-high evaluations-evolutionary algorithms, are used to address optimal energy management in microgrids (MGs) [6]-[13]. A day ahead and short-term level optimization scheduling methodology based on the PSO method is discussed in [14]. Smart microgrids for off-grid rural electricity is discussed in the paper [15]. When power plants are erected in an islanded microgrid, wind energy can be used to provide a significant amount of power in rural areas without access to the bulk electric grid [16]. A multi-period forecasting technique based on automated reinforcement learning is introduced into a standalone microgrid for optimal scheduling [17]. It is suggested that fuel cells and solar panels be used to manage energy in a cost-effective and environmentally responsible manner [18]. An effective energy management for the optimal power in a microgrid is examined in [19]-[26]. An EM structure for a campus

*School of Engineering, Cochin University of Science and Technology, Kochi, Kerala, 682022, India.

[#] Electrical Engineering Department, University of Technology and Applied Sciences, College of Applied Sciences – Sohar, Sultanate of Oman.

[1]Corresponding author:
Email: sarithasngc@gmail.com

microgrid is suggested in [27] to lower operational costs and boost self-consumption from green DGs.

Optimal energy management approach for a DC microgrid is investigated in [28], [29]. An optimal pricing scheme for minimizing the electricity price in a microgrid network is presented [30]. A scenario-based energy management system modelled as a mixed integer linear programming problem is presented in [31] in order to examine the operating behaviour of MGs and subsequently reduce network energy losses. Optimal scheduling technique for a grid connected microgrid with multi-distributed generator units is suggested in [32]. Multi-microgrid energy management systems have a significant role in providing a sustainable, energy-efficient, and reliable green energy supply [33]. In the above literature review, the majority of EM studies/works conducted on microgrid has primarily focused on energy costs and renewable power generation. The stability of the electrical network is crucial for the power system to operate satisfactorily. But this attribute has not been considered in any of the studies cited in the literature review. Considering this research gap, we propose a novel methodology to tackle the issue. The key contributions made by this paper are outlined in the list below.

- An evolutionary algorithmic control strategy for optimal microgrid management in a hybrid system for maximum renewable energy integration is employed.
- This approach ensures a high degree of Renewable energy (RE) penetration into the grid.
- During optimal functioning, system stability is ensured.
- The proposed technique also provides optimum loadability of each load bus connected in the network. Consequently, the possibility of future network extension can be available.
- The developed optimization technique is applied to the campus microgrid (off-grid/on-grid) to evaluate the effectiveness and techno-economic benefits.

The proposed hybrid microgrid system consists of a solar photovoltaic panel, wind generator, biomass, diesel generators, energy storage system, and constant loads. With the integrated microgrid system with storage, this article intends to maximise the penetration of renewable energy sources and actual power loss. In order to analyse the effect of an integrated microgrid on the power grid, this paper investigated the optimal microgrid operation in both off-grid and on-grid modes. A set of evolutionary algorithms are employed for the optimization process. The proposed EM technique ensures optimum generation costs. In off-grid mode, the RE penetration is 87.5% more than the base case, and the generation cost is 555.25 $/hr for 2.52 MW power generation. Whereas in on-grid mode, the RE penetration is 46% more than the base case, and the generation cost is 131,925 $/hr for 1086.11 MW power generation.

The paper is arranged as follows: Section 2 describes the methodology and modeling of the proposed microgrid. Section 3 presents the problem formulation. Section 4 explains the results and discussion. Finally, Section 5 presents conclusions.

2. METHODOLOGY AND MODELING

The main objective of this paper is to maximize the renewable penetration into the grid and, as a result, reduce the cost of power generation for the microgrid in both off-grid and on-grid modes of operation. The Power System Analysis Toolbox (PSAT) in the MATLAB environment is used to simulate the power flow of the microgrid [34].

2.1 Methodology

Figure 1 depicts the functional diagram of the suggested methodology. The picture also shows the model control linkage to the microgrid and power grid. A comprehensive problem formulation, modelling of the wind unit, solar PV, storage, other power generating equipment, loads, and power system are all necessary for the design of algorithm. Stability constraints, in addition to the power system constraints, are also incorporated in the algorithm for ensuring system stability [35].

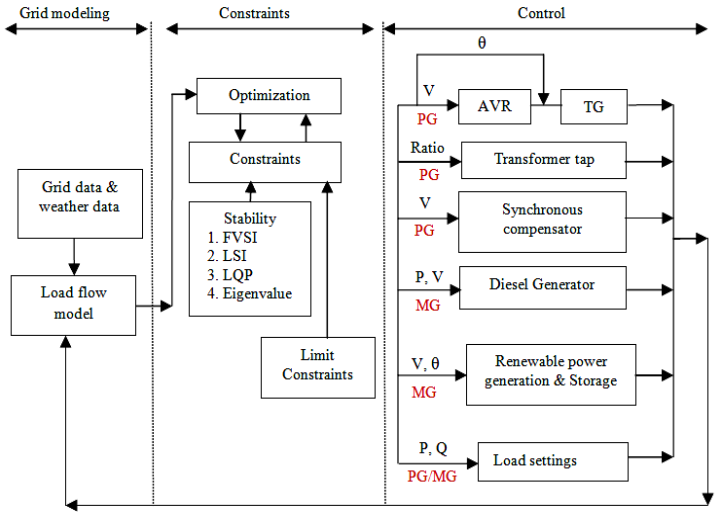

Fig. 1. Control block diagram.

2.1.1 Optimization strategy for microgrid (off-grid mode)

The two goals taken into account for the optimization process are the variable renewable energy (VRE) penetration and power losses. In off-grid mode, the optimization problem is solved using evolutionary algorithms such as Artificial Bee Colony (ABC), Ant Colony Optimization for Continuous Domains (ACOR), Harmony Search (HS), Genetic Algorithm (GA), Differential Evolution (DE), and Particle Swarm Optimization (PSO). Section 4.1 contains a detailed examination of the results.

2.1.2 Optimization strategy for microgrid (on-grid mode)

To assess the efficacy of the optimization approach other than PSO, a methodology based on the NSGA II is employed for the simultaneous optimization of the microgrid in grid-connected mode. NSGA II is a multi-objective, fast, Non-dominated Sorting Genetic Algorithm to optimize each objective's solution simultaneously. It has some significant features such as non-dominated sorting procedure, efficient constraint handling capability, elitist strategy, *etc*., which makes it more attractive in constrained multi-objective optimization platforms. Section 4.2 provides a detailed examination of the results.

2.2 Modeling

A campus electric network (Figure 2) is modeled as a microgrid (MG) and taken as the testbed.

The proposed power system modeling is given in Table 1. The test grid is modeled in PSAT software for simulation.

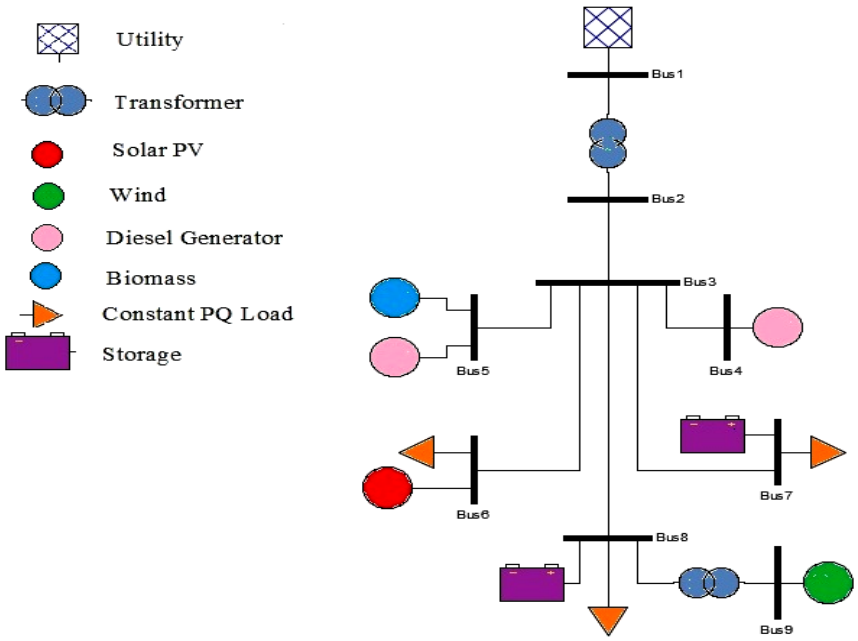

Fig. 2. Single line diagram of the proposed microgrid.

Table 1. Details of power system model.

System Component	Specification
Solar PV	Constant PV model; 1MW
Wind model	Composite distribution; doubly fed induction generator; 2MVA
Battery energy- Storage system	Solid Oxide Fuel Cell; 0.7MW and 0.3MW
Turbine Governor- (TG)	IEEE Type -1; AVR- IEEE Type -2
Generator	Synchronous; Order V, Type II
Load	Constant PQ model

2.2.1 Solar PV model

A constant PV solar photovoltaic generator is employed in this proposed system. This is a centralized SPVG system in which active power injection with voltage magnitude, or reactive power control, is used to describe the buses [36].

2.2.2 Wind unit model

A composite wind model is used in the proposed microgrid. In this model, the resultant wind speed consists of average, ramp, gust, and turbulence components [37]. The turbine generator selected for this wind model is a Doubly Fed Induction Generator (DFIG) with slip ring rotors.

2.2.3 Solid Oxide Fuel Cell (SOFC)

The SOFC is chosen as the storage device in this model. The high operating temperature within this fuel cell allows it to internally reform gaseous fuel, providing

multi fuel capabilities despite its slow start up and thermal stress [38].

3. PROBLEM FORMULATION

This section presents the problem formulation, stability indices, and system constraints employed for the cost optimization of the microgrid and integrated microgrid system.

3.1 Objective Function and Constraints

In order to maximize the power generation from renewable energy sources and reduce the microgrid's power loss in various operating modes, this work tackles the microgrid's power management as a multi-objective issue. Here, the power output from the connected RESs in the microgrid is maximized in order to reduce the overall cost of generation.

The multi-objective optimization issue is stated in the following form:

$$\text{Maximize } f(x) = [\, f_1(x),\ -f_2(x)\,] \tag{1}$$

where, f_1 and f_2 represent RE penetration and system real power losses, respectively. The minus sign in the equation denotes minimization.

3.1.1 Objective 1: Maximize renewable energy penetration

Maximizing the microgrid's renewable power share is the optimization's main goal. The formulation of the evaluation function is:

$$\text{Max } f_1(x,y) = P_R = \sum_{w=1}^{N_w} P_w + \sum_{s=1}^{N_s} P_s \tag{2}$$

here, P_R is the real power generation from renewable sources. The total real power generation from all the wind and solar farms are represented by Pw and Ps, respectively. Where the corresponding wind and solar farm indices are w and s, the total number of wind and solar farms are Nw and Ns, respectively. The term 'x' and 'y 'are the state and algebraic variables.

3.1.2 Objective 2: Minimize real power loss

The secondary goal of the optimization is to minimize the system's real power loss and the problem is formulated as:

$$\text{Minimize } f_2(x,y) = P_L \tag{3}$$

where, P_L is the total real power loss.

The load flow problem is formulated as the solution of a nonlinear set of equations of the form:

$$\begin{aligned} \dot{x} &= f(x,y) \\ 0 &= g(x,y) \end{aligned} \tag{4}$$

here, x is the state variable and y is the vector of algebraic variables (*i.e.* voltage amplitudes (V) and phases (θ)) at the network buses and all other algebraic variables, such as generator field voltages, AVR reference voltages, *etc*. Equations of form 'f' are the differential equations, and of form 'g' are the algebraic equations. Some control and state variables, such as load tap change ratio, are initialised during load flow computations; however, synchronous machines and its regulators are initialised after the load flow computation has been solved. The algorithm used is the Newton-Raphson method based on a distributed slack bus model.

3.2 Power System Constraints:

All the system constraints that are included in the optimization algorithm are discussed in the following section.

3.2.1 Active power balance equation

The active power balance equation in each period is as shown below.

$$\sum P_W + \sum P_S + \sum P_{st,discharge} + \sum P_G = \sum P_D + \sum P_{st,charge} + \sum P_L \tag{5}$$

where, P_W and P_S are the total active power generation from wind and solar units; respectively. P_G is the total active power generation from the generators in the system other than the renewable power sources. $P_{st,charge}$ and $P_{st,discharge}$ are the total charging and discharging power from the storage units, P_D is the total active power demand of the load; and P_L is the total active power loss in the system.

3.2.2 Power constraints of renewable energy sources:

The quantity of power required from renewable energy sources should be less than the quantity of available power from solar and wind power units.

$$0 \le P_D + P_L - \sum_{\substack{i \ne N_W \\ i \ne N_S \\ i=1}}^{N_G} P_{Gi} \le P_W + P_S \tag{6}$$

where, N_W, N_S, and N_G are the numbers of wind units, solar units, and generators other than the renewable power sources, respectively.

3.2.3 Equality power constraints

The equality power constraints in the system can be expressed by a nonlinear load flow equation as:

$$\begin{aligned} P_{Gj} - P_{Dj} &= \sum_{k=1}^{nb} |V_j||V_k||Y_{jk}| \cos(\delta_j - \delta_k - \theta_{jk}) \\ Q_{Gj} - Q_{Dj} &= \sum_{k=1}^{nb} |V_j||V_k||Y_{jk}| \sin(\delta_j - \delta_k - \theta_{jk}) \end{aligned} \tag{7}$$

where, P_{Gj} and Q_{Gj} are the active and reactive power generation at the j^{th} node of the system, P_{Dj} and Q_{Dj} are the active and reactive power demand at the j^{th} node , $|V_j|$ and $|V_k|$ represents voltage magnitude in the j^{th} and k^{th} node, $|Y_{ik}|$ and θ_{jk} are the magnitude and phase angle

of the line admittance between j[th] and k[th] node, δ_j and δ_k are the phase angle of the bus voltage in j[th] and k[th] node; nb denotes the total number of nodes in the network.

3.2.4 Inequality constraints

Both power generation equipment and the distribution system have capacity limits as given in Equation 8.

$$\begin{aligned} P_{Gj\,min} &\le P_{Gj} \le P_{Gj\,max} \\ Q_{Gj\,min} &\le Q_{Gj} \le Q_{Gj\,max} \\ |V_{j\,min}| &\le |V_j| \le |V_{j\,max}| \\ |MVA_{line}| &\le |MVA_{line\,max}| \\ |\delta_{j\,min}| &\le |\delta_j| \le |\delta_{j\,max}| \\ \lambda_{min} &\le \lambda \le \lambda_{max} \end{aligned} \tag{8}$$

here, MVA line is the apparent power flow through the line, and 'λ' is the loading factor.

3.3 Stability Indices

To ensure the system performs consistently and smoothly, a series of system stability parameters, namely line stability, voltage stability, and small signal stability are taken into consideration as constraints in the optimization problem.

3.3.1 Fast voltage stability index (FVSI)

In this work, the fast voltage stability index (FVSI), introduced by Musirin [39], which is based on the concept of power flow across a single line is employed for the stable operation of the system. This index can be used to assess the voltage stability state of each line in a power system. For the transmission line, let '*j*' and '*k*' be the sending and receiving end buses, then the voltage stability index is calculated as:

$$FVSI_{jk} = \frac{4Z^2 Q_k}{V_j^2 X} \tag{9}$$

where *X* and *Z* denote the transmission line's reactance and impedance. V_j is the sending end bus voltage, and Q_k is the receiving end's reactive power. For a stable system operation, the FVSI value of each line must be less than 1.00. A value greater than 1.00 on the stability index indicates a voltage collapse condition.

3.3.2 Line stability factor (LSF)

LSF, which is denoted as (LQP) and represented by Equation 9 is used to evaluate network stability. For the system to remain stable, LQP's value must be less than 1.00 [39] and this index predicts any overload condition of the power lines. By taking 'j' and 'k' as sending end and receiving end bus; the line stability factor can be expressed as:

$$LQP_{jk} = 4\left(\frac{X}{V_j^2}\right)\left(\frac{X}{V_j^2}P_j^2 + Q_k\right) \tag{10}$$

where, P_j is the real power at the sending end. For a stable system, LQP must be less than 1.

3.3.3 Line stability index (LSI)

For a two-bus electrical network, the stability of the line can be found using the line stability index (LSI) [40]. In order to maintain a system stable, LSI value must be less than 1.00; if it is greater than 1, the system as a whole loses stability, leading to voltage collapse. The index is given by:

$$LSI_{jk} = \frac{4Q_k X}{\left[|V_j| \sin(\theta - \delta)\right]^2} \tag{11}$$

where θ is the line impedance angle and $\delta = \delta_j - \delta_k$.

3.4 Small Signal Stability

Equation 4 depicts the power system's differential algebraic equations (DAE) model. The evaluation of the state matrix AS is used for the eigenvalue analysis. The complete Jacobian matrix AC, which is defined by the linearization of the DAE system equations at the equilibrium point, is modified to produce the state matrix AS.

$$\begin{bmatrix} \Delta\dot{x} \\ 0 \end{bmatrix} = \begin{bmatrix} f_x & f_y \\ g_x & g_y \end{bmatrix} \begin{bmatrix} \Delta x \\ \Delta y \end{bmatrix} = [A_c] \begin{bmatrix} \Delta x \\ \Delta y \end{bmatrix} \tag{12}$$

The small signal stability model of the proposed microgrid can be expressed as [37]:

$$\Delta\dot{x} = A_c \Delta_x \tag{13}$$

where, x is the state vector variable, A_c is the Jacobian matrix, and A_S is the state matrix which is represented as

$$A_s = f_x - f_y g_y^{-1} g_x \tag{14}$$

where, f_x, f_y, g_x, and g_y are the Jacobian matrices given in Equation 12.

The eigenvalues in the S domain can be computed using the state matrix in Equation 14, and the power system is said to be stable if the real component of all the eigenvalues are negative.

3.5 Generation Cost Calculation

The quadratic fuel cost function that is used for conventional generators is taken as a linear function for the generating sources in the proposed system, and the cost coefficients are determined using unit costs available in [41] and [42]. The cost coefficients a, b, and c are incorporated into the optimization algorithm to determine the generation cost, and the data is given in Table 2.

Table 2. Cost coefficient data.

Source	a ($/MW^{2}h)	b ($/MWh)	c ($/h)
Hydro power unit	0	120	480
Solar power unit	0	13.6	27.2
Wind power unit	0	6.016	23.47
Storage unit	0	4	4

4. RESULTS AND DISCUSSION

The power flow of the microgrid (off-grid and on-grid) is carried out using the Power System Analysis Toolbox

(PSAT) in the MATLAB environment, and the PSAT model (base case) of the microgrid is embedded in the optimization algorithm. The power system constraints and stability requirements are incorporated into the algorithm during the optimization process. The loading parameter is controlled in the proposed strategy to feed as much renewable energy as possible into the microgrid. The algorithms comparison of the two test cases (off-grid and on-grid mode) of the proposed microgrid is discussed in this section.

4.1 Case I: Algorithm Comparison of Microgrid in Off-Grid Mode

In off-grid mode, PSO, a swarm intelligence tool, is applied to optimize renewable penetration and power loss while concurrently optimizes the generation cost of the proposed microgrid system. Table 3 compares the performance of various evolutionary optimization techniques used in solving the proposed energy management problem.

From the comparison statement, it is clear that the PSO approach provides the best combination of generation cost and renewable energy share. Furthermore, the active power loss in the optimal case is 8.73%, whereas it is 10.6% in the base case. As a result, for the given optimization problem, the PSO strategy is chosen, and the result analysis is explained in the preceding section.

4.1.1 Result analysis of microgrid (off-grid mode)

In this section, the power generation from various sources, bus voltages, stability analysis, and power flow during the optimal and base cases of the microgrid are discussed. The microgrid can absorb more power from the associated RESs in the optimal scenario since the loadability of the entire system is boosted without affecting system stability. Table 4 shows the microgrid's optimal outcome analysis in off-grid mode.

Table 4 illustrates that the increase in load demand is balanced by the renewable energy contribution, not by the system's conventional power source. In this optimization process, the real power loss is also minimized. In optimal operation, the renewable share increases by 0.0105 p.u., as shown in Table 4. As a result, we may deduce that optimal operation can enhance renewable energy shares. Applying the proposed optimal technique, the generation cost in the base case is 554.73 $/hr for 1.32MW, whereas in the optimal case, it comes to 555.25 $/hr for 2.52 MW.

Table 3. Comparison of Evolutionary algorithms used in off -grid mode

Parameter	Max Penetration						
	Number of iterations		30		Population size		20
	Base case	ABC	ACOR	DE	GA	HS	PSO
Active Power generation in p.u	0.0132	0.0251	0.0251	0.025	0.0252	0.0252	0.0252
Active powerloss in p.u	0.0014	0.0022	0.0022	0.0022	0.0022	0.0022	0.0022
Active load in p.u	0.0118	0.0229	0.0229	0.0228	0.023	0.023	0.023
RE (Solar+wind) penetration (MW)	1.2	2.29	2.26	2.27	2.30	2.31	2.25
Generation Cost($/hr)	554.73	555.66	555.35	555.46	555.8	555.92	555.25

Table 4. Optimal result analysis of microgrid in off-grid mode.

Scenario	Active power generation from various sources (in p. u.)			Total active load in p. u.	Total active power generation in p. u.	Total active power loss in p. u.
	(Solar +Wind) Renewable share	Conventional source	Storage			
Base case	0.012	0.00082	0.00035	0.0118	0.0132	0.0014
Optimal case	0.0225	0.0001	0.0026	0.0230	0.0252	0.0022
Increment (+/-)	0.0105	-0.00072	0.00225	0.0112	0.0120	0.0008

The voltage analysis of the microgrid for the base case, and the optimal case is as shown in Figure 3.

The graph shows that all bus voltages are between 0.9 and 1.1 p.u., which is the acceptable limit. So, it is evident that using the proposed optimal control strategy, the voltage level can be maintained within the limit while hosting more load and renewable share to the existing grid. By adjusting the loading factor, the optimum safe loading in each bus may be determined, resulting in a higher renewable share from RESs connected to the microgrid. Figure 4 displays the active power flow during the base case and optimal case. This graph can be used for identifying the overloaded lines in the network. The most heavy-laden lines in this scenario are lines 8-3 and 9-8.

The system stability in optimal case is guaranteed by the insertion of stability criteria in the optimization problem. Figure 5 shows that the FVSI/LSI has the maximum value, which is only 0.15. (Approx. 1/6th of the limit), indicating that the proposed microgrid system is stable in the optimal case.

Figure 6 represent the eigenvalues of the microgrid system for the base case and optimal case. Due to concerns about analytical clarity, the higher order eigenvalues are excluded. The graph clearly shows that there is no appreciable difference between the base and optimal cases. The position of eigenvalues (real part of every eigenvalue is on the left side of the S plane) in Figure 6 illustrates the stability constrained plot for the microgrid, demonstrating that system stability is maintained for optimal operation of the system. The features of Figures 5 and 6 indicate the proposed controller's ability to preserve grid stability under optimal condition and preventing bus or line overloading.

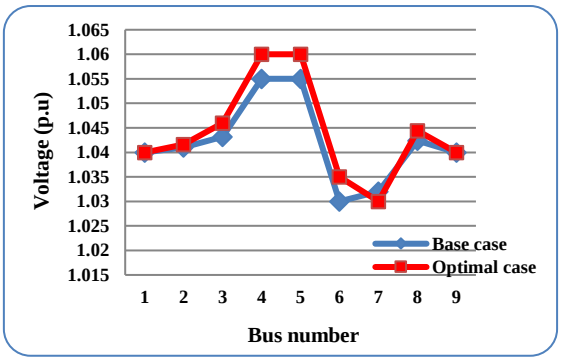

Fig. 3. Voltage profile of microgrid.

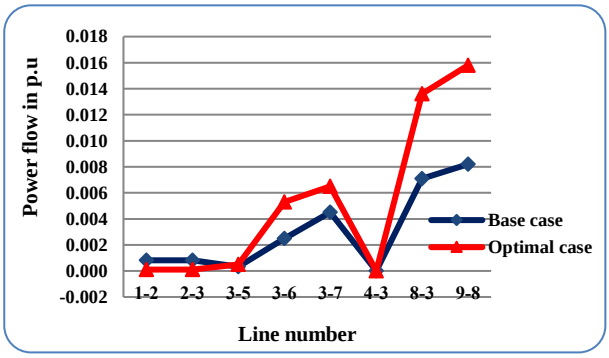

Fig. 4. Active power flow profile in microgrid.

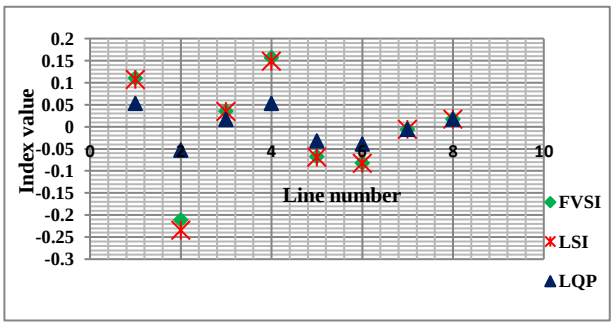

Fig. 5. Stability indices of microgrid system.

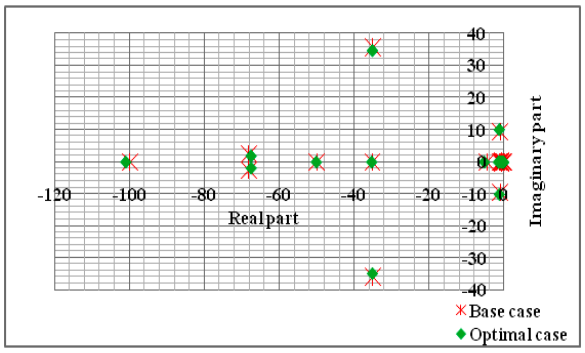

Fig.6. Eigenvalue stability analysis of microgrid.

4.2 Case II: Algorithm Comparison of Microgrid in Grid Connected Mode

The proposed microgrid is integrated into the Power Grid (PG), and Figure 7 shows the grid-connected system.

The power grid (PG) in this model is the central area network of the Indian (Kerala) power system. The conventional sources in the power grid have installed capacities of 780MW, 220MW, 100MW, and 50MW, respectively.

The comparative report of the optimization results for an integrated microgrid employing the NSGA II approach and PSO are shown in Table 5. In this aspect, the NSGA II method seems more promising than PSO in terms of achieving the best possible outcomes for RE penetration, generating cost, and power loss. As can be shown, the increase in loadability from 951.18 MW in the base case to 1040.57 MW in the optimal case (9.4%) causes the RE penetration to increase from 1.96 MW to 2.86 MW (45.92%) in the NSGA II approach. In the base case, generating 985.08 MW of electricity costs $119,966 per hour, whereas in the optimal scenario, producing 1086.11 MW costs only $131,925. As a result, even though it is a minor reduction, the cost per MWhr is lower in the optimal scenario than in the base case. The system will be more cost-effective when a powerful microgrid is linked with the electrical grid and with multi- microgrid integration.

The power loss as a percentage in the base scenario is 3.44, whereas in the optimal mode, it is 4.19. This increase is entirely reasonable given that the microgrid is interconnected with a power grid and that the overall system loss will increase relative to the base case when power flow increases in the optimal scenario.

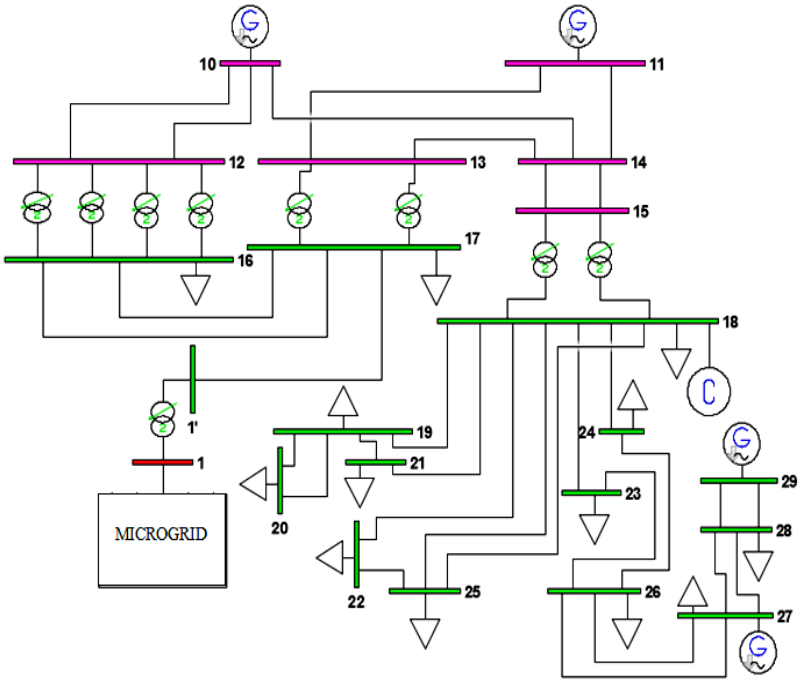

Fig. 7. Line diagram of microgrid- power grid integration.

Table 5. Algorithm comparison report of Integrated microgrid (on-grid) mode.

Parameter	Unit	Base Case	Max. Penetration	
			NSGA	PSO
Total generation	MW	985.08	1086.11	1086.32
Active power- loss	MW	33.9	45.54	46.02
Total load	MW	951.18	1040.57	1040.29
RE penetration (Solar+Wind)	MW	1.96	2.86	2.84
Generation Cost	$/hr	1,19,966	1,31,925	1,31,948

Table 6. Optimal result analysis of integrated microgrid (on-grid mode operation).

Scenario	Power generation (MW)			Total load (MW)	Total generation (MW)	Power exchange (MW) through the tie-line(1-1')	Active power loss (MW)
	(Solar + wind) Renewable	Conventional source	Storage				
Base case	1.96	983.11	0.01	951.18	985.08	0.46	33.9
Optimal case	2.86	1082.7	0.56	1040.57	1086.11	2.01	45.54
Increment (+/-)	0.9	99.59	0.55	89.39	101.03	1.55	11.64

4.2.1 Result analysis of microgrid (on-grid mode)

This section covers the analysis of integrated microgrid system in optimal operation. Table 6 gives the active power contributions of various sources in the integrated system in both the base and the optimal cases.

Table 6 demonstrates that in optimal operation, the conventional power share decreases (from 99.8% of total generation in the base case to 99.68 % in the optimal case) while the renewable power share increases (0.19 percent of total generation in the base case to 0.26 percent in optimal case). In this scenario, the percentage figure is less due to the microgrid's limited capacity compared to the power grid, and the share of renewable energy is controlled by the power grid's and microgrid's capacity and system factors.

As a result of the microgrid's integration into the power grid, conventional power generation is reduced while renewable power is increased, which has significant economic benefits and helps mitigate climate change. Renewable energy will play a significant part in an integrated microgrid system.

4.2.2 Voltage analysis

This section explains the voltage analysis of the integrated microgrid – main grid system. Figure 8 shows the bus voltages in the integrated microgrid system in the base and optimal scenarios, and it clearly indicates that, all bus voltages are in the acceptable range (0.9 p.u. to 1.1 p.u.) in the optimal scenario of the grid connected mode.

In the optimal case, the lowest voltage level occurs at bus #27, and the highest one is at bus #18. Here, the bus voltage is regulated by the grid's reactive power management.

The bus voltage study shows that integrating the microgrid into the main grid (power grid) enhances bus voltage (bus #10-29). Due to microgrid-maingrid integration the voltage improvement in base case and optimal case is found to be almost 65% and 90% of the buses respectively. This result shows that main grid bus voltage may be improved by the action of microgrid integration into the main grid. So a powerful microgrid can support the main grid to some extent. The findings also show that when the electrical grid is operating at its optimal loading margin, bus voltages will improve significantly. Considering this system phenomenon, it is clear that optimal operation of integrated grid enhances its bus voltages.

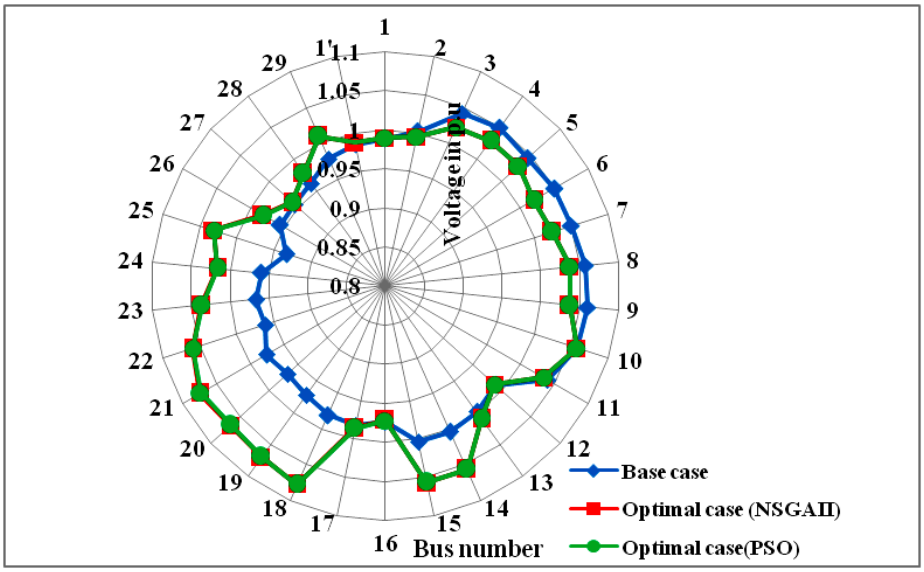

Fig. 8. Bus voltage profile during on-grid mode.

4.2.3 Power flow and loadability analysis

Figure 9 shows the active power flow through the lines during the microgrid integration.

In the grid connected mode, main grid line 10-14 is the most heavily loaded in both base and optimal cases. Line 1-1' in the power flow graph shows positive power, which indicates active power flow is from bus #1 (microgrid) to bus #1' (main grid). In this scenario, the excess power generated by the RESs flows to the main grid (power grid) through the tie line 1-1'. This phenomenon shows that power exchange is made possible by grid integration.

Grid integration and its optimal operation will improve power flow in the grid lines. Nearly 75 percent of microgrid lines and 78 percent of the main grid lines (Figures 10 and 11) have improved power flow as a result of grid integration (The table is ignored due to space issue).

Thus, the grid integration scenario shows that a robust microgrid may support the main grid in terms of voltage augmentation, power exchange and thereby assure a reliable and quality power supply.

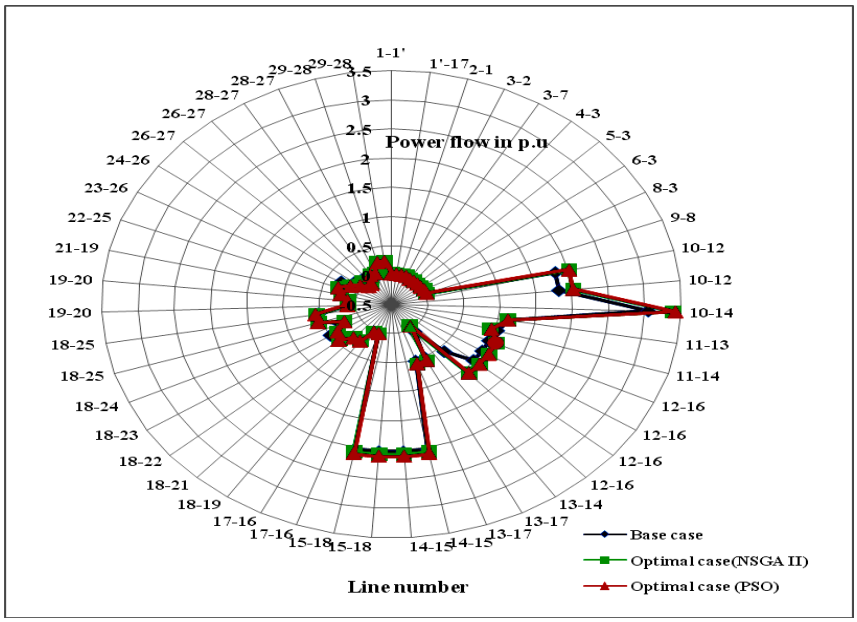

Fig. 9. Active power flow during grid connected mode.

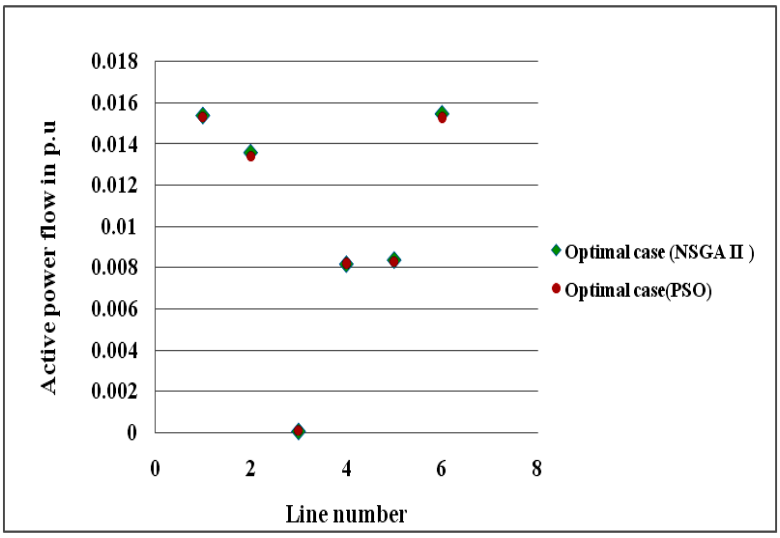

Fig. 10. Active power flow increment in microgrid lines.

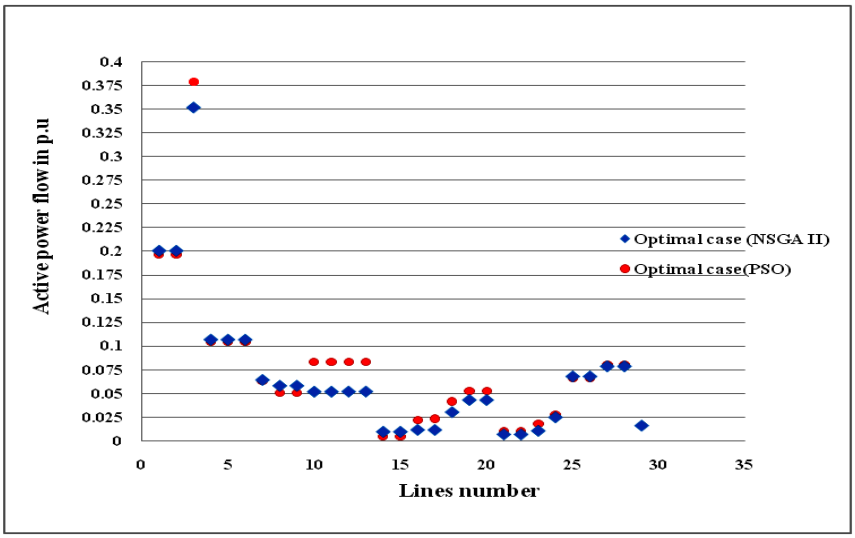

Fig. 11. Active power flow increment in main-grid lines.

In this proposed method, loadability of the system is increased to achieve more renewable penetration, and thereby the generation cost of the grid system can be optimized to a great extent. The optimum load demand at each load bus has been achieved by the control strategy applied in the system and the load profile is furnished as shown in Figures 12 and 13.

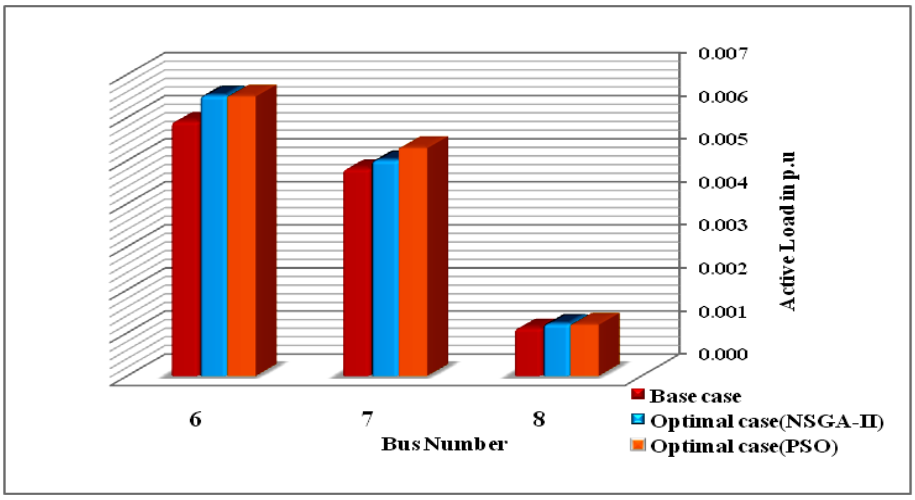

Fig. 12. Load profile of microgrid during integration.

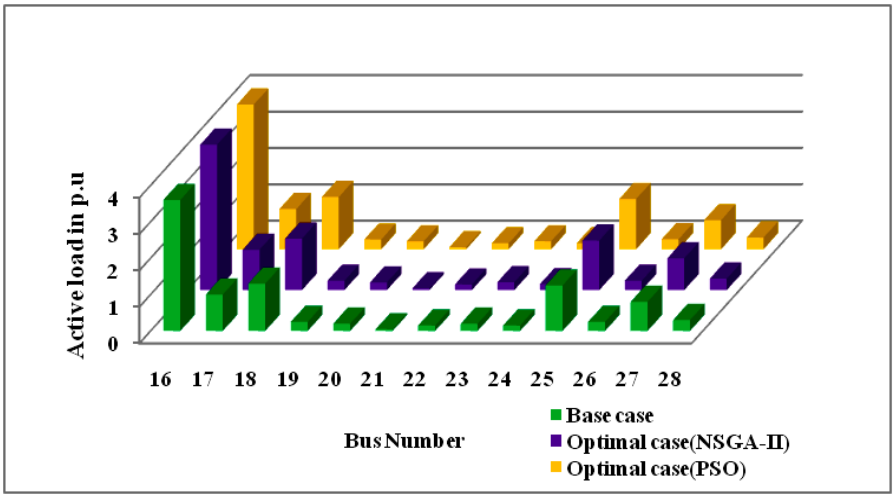

Fig. 13. Load profile of main grid during integration.

Almost 88% of the load buses in the system shows load increment and this ensures that the loadability of the entire system is maximized without affecting the system stability and the load increment is found to be 9.4% more than the base case load.

In the optimal scenario, the power transfer within the microgrid and power grid (line 1-1') are 0.0201 p.u. (2.01 MW) by the NSGA II method and 0.0199 p.u. (1.99 MW) by the PSO method. All of these power flow evaluations show that grid integration and optimal loading can improve system performance.

4.2.4 Stability Analysis

This section explains the system stability analysis during the optimal operation. Eigenvalue stability approach ensures the integrated system's stability. Figure 14 represent the eigenvalues of the integrated microgrid system for the base case and optimal case. Due to concerns over analytical lucidity, the higher-order eigenvalues are not considered. The graph makes it obvious that, aside from one value, where the eigenvalue (real part) position shifts more towards the left side than the base case to imply higher stability, there is no discernible change in either situation. In both scenarios, the real part of each eigenvalue is on the left-hand side of S plane, demonstrating the system's stability in a high degree of renewable penetration. The system is more secure if the eigenvalues are far away from the origin and towards the left half of the S plane.

The stability indices FVSI, LSI, and LQP, ensure the system's stability in the optimal operation of the integrated microgrid system. The aforementioned grid stability indices can be used to ensure grid stability in various modes of operation. Figure 15 demonstrates the analysis of stability indices in the proposed system's on-grid mode optimal operation.

All of the stability index values are less than 1.00 in both optimization methods, ensuring network stability. These figures ensure that no bus or line is overloaded while operating in on-grid mode optimal operation. The highest stability index value (FVSI and LSI) for both optimization methods is recorded in line #40 and is only less than 0.25 (one-fourth of the maximum limit).

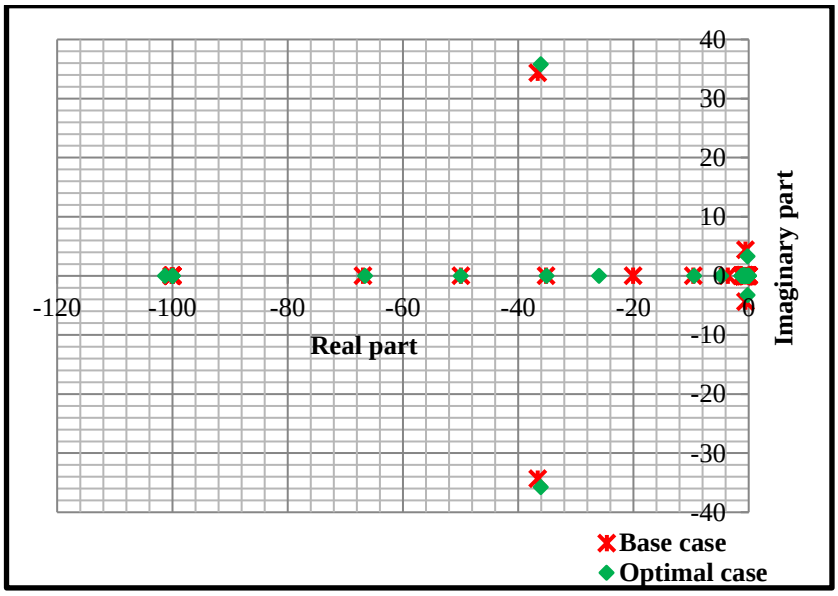

Fig. 14. Eigenvalues of the system during on-grid mode.

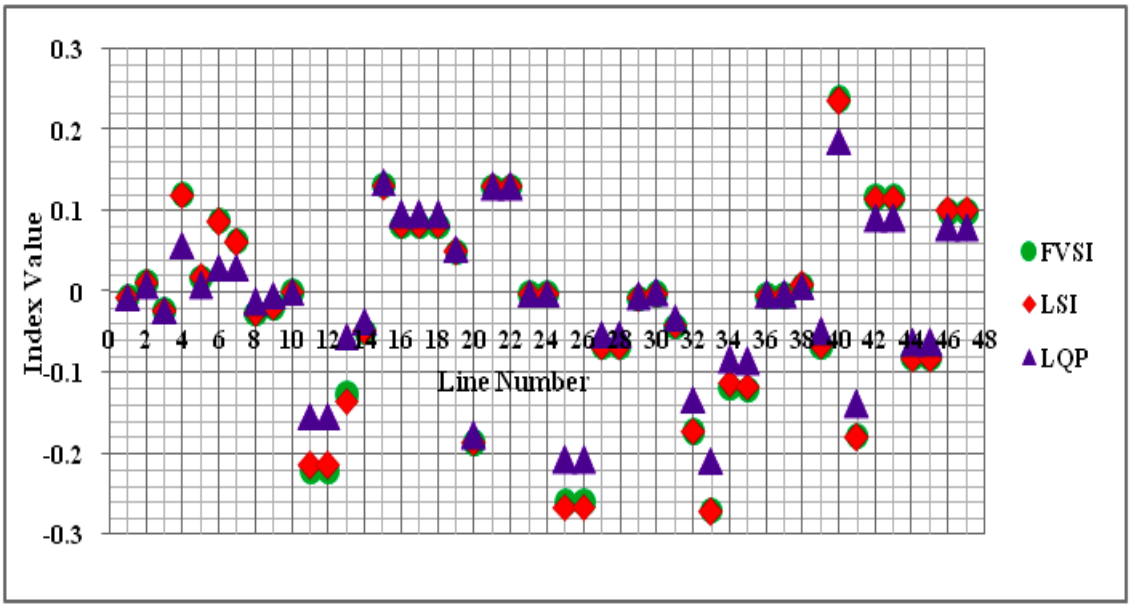

Fig. 15. Stability Indices of the system during on- grid mode.

5. CONCLUSIONS

This paper proposes a novel optimum control method for microgrid energy management in both the off-grid and on-grid modes of operation. The major goal is to maximize the penetration of renewable energy sources while preserving system stability in order to manage generation costs effectively for the microgrid system. An optimal control strategy based on swarm intelligence has been employed to optimize RE penetration and power loss in a campus microgrid. For the grid-connected mode, the NSGA II method is used and validated with PSO. The suggested optimization methods discussed in this paper made it possible to find the best solution in a highly effective and efficient way. A cost-effective power control (in both off-grid and grid-connected modes) of the suggested microgrid system is achieved by optimizing renewable energy penetration and power loss. Furthermore, the goal is achieved by optimum safe loading without breaching system limits or compromises stability.

The conclusion reached from the optimization findings can be summarized as follows:

- In the optimal case, the microgrid's loadability (in off-grid mode) is increased by 94.9%, resulting in an additional 87.5% of renewable energy penetration and a decrease in active power loss from 10.6% (base case) to 8.73%.
- In on- grid mode, the loadability of the entire system is increased by 9.4% in optimal case, leading to an additional 46% renewable energy penetration, while the active power loss of the integrated microgrid system is 3.44% in the base case and only 4.2% in the optimal case.
- More power share from RESs results in significant economic benefits and climate change mitigation.
- Grid integration offers increment in renewable power share, voltage enhancement, and power exchange through the network.
- Grid-connected microgrid can support the main grid to some extent.
- The loadability of each load bus can be evaluated, allowing the system's future expansion potential to be assessed.
- Power system constraints, small-signal stability, voltage, and line stability indices included in the optimization ensures stable system operation.

These findings appear to be promising for microgrid power management in various modes of operation and especially in the grid modernization in the electric power sector. The proposed optimization technique can be extended for real-time power management in microgrids, as well as simultaneous optimization of the multi-microgrid integrated systems.

REFERENCES

[1] Zehir M.A., Batman A., Sonmez M.A., Font A. ,and Tsiamitros D., 2016. Impact of renewable based microgrid supply / demand profiles on low voltage distribution networks. *Energy Procedia* 103: 231–236.

[2] Heydt G.T. Chowdhury B.H., Crow M.L., Haughton D., Keifer B.D., Meng F., and Sathyanarayana B.R., 2012. Pricing and control in the next generation power distribution system. *IEEE Transaction on Smart Grid* 3(2): 907–914.

[3] Pena A.L., Arriaga I.P., and Linares P., 2012. Renewables vs. energy efficiency : the cost of carbon emissions reduction in Spain. *Energy Policy* 50: 659–668.

[4] Bano T. and K.V.S. Rao. 2016. The effect of solar PV module price and capital cost on the levelized electricity cost of the solar PV power plant in the context of India. In *Proceedings of the 2016 Biennial IEEE International conference on Power and Energy systems: Towards Sustainable Energy (PESTSE).* Bengaluru, 21-23 January. India: IEEE.

[5] Singh S., Gao D.W., and Giraldez J., 2017. Cost analysis of renewable energy- based microgrids. In *Proceedings of the 2017 North American Power*

Symposium(NAPS). Morgantown, WV, 17-19 September. USA: IEEE.

[6] Shadmand M.B and R. Balog. 2014. Multi-objective optimization and design of photovoltaic-wind hybrid system for community. *IEEE Transactions on Smart Grid* 5(5): 2635-2643.

[7] Aghajani G. and N. Ghadimi. 2017. Multi-objective energy management in a micro- grid. *Energy Reports* 4: 218–225.

[8] Indragandhi V., Logesh R., Subramaniyaswamy V., Vijayakumar V., Patrick S., and Lorna U., 2018. Multi-objective optimization and energy management in renewable based AC / DC microgrid *Computer and Electrical Engineering* 70: 179-198.

[9] Azaza M. and F. Wallin. 2017. Multi objective particle swarm optimization of hybrid microgrid system : A case study in Sweden. *Energy* 123:108–118.

[10] Bilil H., Aniba G., and Maaroufi M., 2014. Multi objective optimization of renewable energy penetration rate in power systems. *Energy Procedia* 50: 368–375.

[11] Conti S., Nicolosi R., Rizzo S., and Zeineldin H.H., 2012. Optimal dispatching of distributed generators and storage systems for MV islanded microgrids. *IEEE power Transaction on Power Delivery* 27(3): 1243–1251.

[12] Zhang X., Sharma R., and He Y., 2012. Optimal energy management of a rural microgrid system using multi-objective. *IEEE PES Innovative Smart Grid Technologies (ISGT)*: 1–8.

[13] Duais A., Osman M., Shullar M.H., and Abido M.A., 2021. Optimal real-time pricing-based scheduling in home energy management system using genetic algorithms. In *proceedings of the IEEE 4th International Conference on Renewable Energy and Power Engineering (REPE)*. Beijing, 09-11 October, China: IEEE.

[14] Wang X. and Y. Zheng. 2020. Energy management of microgrid based on day-ahead and short-term optimization. *International Journal Simulation and Process Modelling* 15(4):311-321.

[15] Nnaji E.C., Adgidzi D., Dioha M.O., Ewim D.R.E., and Huan Z., 2019. Modelling and management of smart microgrid for rural electrification in sub-Saharan Africa : The case of Nigeria. *The Electricity Journal* 32(10).

[16] Hamed B., Gao W., Wu Z., and Li. Y., 2013. Optimal energy management of wind power generation system in islanded microgrid system. In *Proceedings of the 2013 North American Power Symposium (NAPS)*. Manhattan, KS, 22-24 September. USA: IEEE.

[17] Li Y., Wang R., and Yang Z., 2021. Optimal scheduling of isolated microgrids using automated reinforcement learning-based algorithm. *IEEE Transaction on Sustainable Energy* 13(1): 159 – 169.

[18] Nishiura E., Matsuhashi R., Ferrão P., and Fournier J., 2017. Study for optimal energy management system in houses collectively receiving electricity at low. *Energy Procedia* 141: 479–483.

[19] Li H., Eseye A.T., Zhang J., and Zheng D., 2017. Optimal energy management for industrial microgrids with high-penetration renewable. *Protection and Control of Modern Power Systems* 2(12): 1–14.

[20] Chauhan A. and R.P. Saini. 2013. Renewable energy based power generation for stand-alone applications: A review. In *Proceedings of 2013 International Conference on Energy Efficient Technologies for Sustainability*. Nagercoil, 10-12 April. India: IEEE.

[21] Giraldo J.S., Castrillon J.A., Lopez J.C., Rider M.J., and Carlos A.C., 2019. Microgrids energy management using robust convex programming. *IEEE Transaction on Smart Grid* 10(4): 4520 – 4530.

[22] Delfino F., Ferro G., Robba M., and Rossi M., 2019. An energy management platform for the optimal control of active and reactive power in sustainable microgrids. *IEEE Transactions on Industry Application* 55(6): 7146 -7156.

[23] Quoc-tuan T., Ngoc Luu A., and Nguyen L.T., 2016. Optimal energy management strategies of microgrids. In *Proceedings of IEEE Symposium Series on Computational Intelligence (SSCI)*, Athens, 06-09 December. Greece: IEEE.

[24] Bagheri-Sanjareh M., 2020. Energy management of islanded microgrid by coordinated application of thermal and electrical energy storage systems. *International Journal of Energy Research* 45(4): 5369-5385.

[25] Murty V.V.S.N. and A. Kumar. 2020. Multi-objective energy management in microgrids with hybrid energy sources and battery energy storage systems. *Protection and Control of Modern Power Systems* 5(1):1–20.

[26] Fathy A., Alanazi T.M., Rezk H., and Yousri D., 2022. Optimal energy management of micro-grid using sparrow search algorithm. *Energy Reports* 8: 758–773.

[27] Javed H., Muqeet H.A., Shehzad M., Jamil M., Khan A.A., and Guerrero J.M., 2021. Optimal energy management of a campus microgrid considering financial and economic analysis with demand response strategies. *Energies* 14(24): 8501.

[28] Park K., Lee W., Wonpoong P., and Lee W., 2019. Optimal energy management of DC microgrid system using dynamic optimal programming. *IFAC- Papers on Line* 52(4):194–199.

[29] Wang P., Wang W., Meng N., and Xu D., 2018. Multi-objective energy management system for DC microgrids based on the maximum membership degree principle. *Journal of modern Power Systems and Clean Energy* 6(4): 668–678.

[30] Hossain M., Tushar K. and Assi C., 2017. Optimal energy management and marginal cost electricity pricing in microgrid network. *IEEE Transactions on Industrial Informatics* 13(6): 3286 – 3298.

[31] Erenoglu A.K., Sengor I., Erdinç O., Taşcıkaraoglu A., Tas A., and Catalão, J.P.S., 2022. Optimal energy management system for microgrids considering energy storage, demand response and renewable power generation. *International Journal of Electrical Power and Energy Systems*. 136(2022):

[32] Raghav L.P., Kumar R.S., Raju D.K., and Singh A.R., 2021. Optimal energy management of

microgrids using quantum teaching learning based algorithm. *IEEE Transactions on Smart Grid* 12(6): 4834–4842.

[33] Liu N., Voropai N., and Xu D., 2021. Multi-microgrid Energy Management Systems : Scheduling Strategies. *Journal of Modern Power Systems and Clean Energy* 9(3): 463–476.

[34] Saritha K.S, Sasidharan S., and Usha N., 2018. A generalized setup of a campus microgrid - A case study. In *Proceedings of the IEEE Conference (ICECDS).*Chennai, 1-2 August. India: IEEE.

[35] Sreedharan S., Joseph T., Vishnu J., Veni C., Joseph S., and Vipin D., 2020. Power system loading margin enhancement by optimal STATCOM integration- A case study. *Computers and Electrical Engineering* 81(2020).

[36] Tamimi B. and C. Canizares. 2013. System stability impact of large-scale and distributed solar photovoltaic generation : the case of Ontario, Canada. *IEEE Transactions on Sustainable Energy* 4(3): 680-688.

[37] Milano, F., 2013. *Power System Analysis Toolbox documentation for PSAT*, version 2.1.8: 2013.

[38] Wang C. and. M.H. Nehrir. 2007. A physically based dynamic model for solid oxide fuel cells. *IEEE Transactions on Energy Conversion* 22(4): 887–897.

[39] Musirin I. and T.K.A. Rahman. 2002. Novel fast voltage stability index (FVSI) for voltage stability analysis in power transmission system. In *Proceedings of Student Conference on Research and Development,* Shah Alam Malaysia, 17 July. Malaysia: IEEE.

[40] Moghavvemi M. and F.M. Omar. 1998. Technique for contingency monitoring and voltage collapse prediction. IET Digital Library . *IEE Proceeding on Generation, Transmission and Distribution* 145(6): 634-640.

[41] Power Generation Costs- IRENA, world wide web: https://www.irena.org/costs/Power Generation-Costs.

[42] Nikmehr N. and S.N. Ravadanegh. 2015. Optimal power dispatch of multi-microgrids at future smart distribution grids. *IEEE Transactions on Smart Grid* 6(4): 648-1657.